Geomechanics and Engineering, *Vol. 30, No. 1 (2022) 11-26*
https://doi.org/10.12989/gae.2022.30.1.011

Prediction of squeezing phenomenon in tunneling projects: Application of Gaussian process regression

Majid Mirzaeiabdolyousefi[1a], Arsalan Mahmoodzadeh[*2], Hawkar Hashim Ibrahim[3b], Shima Rashidi[4c], Mohammed Kamal Majeed[5d] and Adil Hussein Mohammed[6e]

[1]*Department of Mining, Petroleum & Geophysics Engineering, Shahrood University of Technology, Iran*
[2]*Rock Mechanics Division, School of Engineering, Tarbiat Modares University, Tehran, Iran*
[3]*Department of Civil Engineering, College of Engineering, Salahaddin University-Erbil, 44002 Erbil, Kurdistan Region, Iraq*
[4]*Department of Computer Science, College of Science and Technology, University of Human Development, Sulaymaniyah, Kurdistan Region, Iraq*
[5]*Information Technology Department, Faculty of Science, Tishk International University (TIU), Erbil, Kurdistan Region, Iraq*
[6]*Department of Communication and Computer Engineering, Faculty of Engineering, Cihan University-Erbil, Kurdistan Region, Iraq*

(Received February 10, 2022, Revised May 22, 2022, Accepted May 30, 2022)

Abstract. One of the most important issues in tunneling, is the squeezing phenomenon. Squeezing can occur during excavation or after the construction of tunnels, which in both cases could lead to significant damages. Therefore, it is important to predict the squeezing and consider it in the early design stage of tunnel construction. Different empirical, semi-empirical and theoretical-analytical methods have been presented to determine the squeezing. Therefore, it is necessary to examine the ability of each of these methods and identify the best method among them. In this study, squeezing in a part of the Alborz service tunnel in Iran was estimated through a number of empirical, semi- empirical and theoretical-analytical methods. Among these methods, the most robust model was used to obtain a database including 300 data for training and 33 data for testing in order to develop a machine learning (ML) method. To this end, three ML models of Gaussian process regression (GPR), artificial neural network (ANN) and support vector regression (SVR) were trained and tested to propose a robust model to predict the squeezing phenomenon. A comparative analysis between the conventional and the ML methods utilized in this study showed that, the GPR model is the most robust model in the prediction of squeezing phenomenon. The sensitivity analysis of the input parameters using the mutual information test (MIT) method showed that, the most sensitive parameter on the squeezing phenomenon is the tangential strain ($\varepsilon_{\theta}^{\alpha}$) parameter with a sensitivity score of 2.18. Finally, the GPR model was recommended to predict the squeezing phenomenon in tunneling projects. This work's significance is that it can provide a good estimation of the squeezing phenomenon in tunneling projects, based on which geotechnical engineers can take the necessary actions to deal with it in the pre-construction designs.

Keywords: artificial neural network; empirical; Gaussian process regression; semi-empirical and theoretical-analytical methods; squeezing phenomenon; support vector machine

1. Introduction

Tunnel squeezing is one of the major geological disasters that often occur during the construction of tunnels in weak rock masses subjected to high in situ stresses. It could cause shield jamming, budget overruns, and construction delays and could even lead to tunnel instability and casualties. Therefore, an accurate prediction or identification of tunnel squeezing is extremely important in the design and construction of tunnels. (Ghasemi and Gholizadeh 2018). Until now, the squeezing potential of rock masses located on the tunnels route has been evaluated by various methods. The most important of these methods are empirical methods, such as, Singh *et al.* (1992) and Goel *et al.* (1995), semi-empirical methods, such as, Aydan *et al.* (1993), Jethwa *et al.* (1984) and Hoek and Marinos (2000), and International Society for Rock Mechanics (ISRM). Empirical methods are based on two parameters of rock-mass (Q-system) and tunnel depth. Semi-empirical methods provide indicators for determining the squeezing potential and predict this potential by using the expected deformations around the tunnel in a hydrostatic stress field. Theoretical-analytic methods include all methods based on closed solutions and numerical methods.

Recently machine learning (ML) techniques have been applied for landslide displacement (Grelle and Guadagno 2012, Rohmer and Foerster 2011, Liu *et al.* 2014),

∗Corresponding author, M.Sc.,
E-mail: arsalan.mahmoodzadeh@uoh.edu.iq
[a]M.Sc.
E-mail: mirzae.majid@yahoo.com
[b]M.Sc.
E-mail: hawkar.ibrahim@su.edu.krd
[c]M.Sc.
E-mail: shima.rashid@uhd.edu.iq
[d]M.Sc.
E-mail: mohammed.kamal@tiu.edu.iq
[e]M.Sc.
E-mail: adil.mohammed@cihanuniversity.edu.iq

ISSN: 2005-307X (Print), 2092-6219 (Online)

surrounding rock deformation (Feng *et al.* 2004, Wang *et al.* 2012), tunnel face stability (Li *et al.* 2021), estimation of tunnel support patterns (Liu *et al.* 2021), tunnel cost and duration prediction (Mahmoodzadeh *et al.* 2022), tunnel geology evaluation (Bai *et al.* 2021), prediction of flow ability of soft soil (Xiang *et al.* 2021), water inflow prediction in tunnel construction (Li *et al.* 2017), and other geotechnical engineering problems. These methods have shown the potential ability to analyze the problems in engineering projects (Liu *et al.* 2006, Pal and Deswal 2010, Yuan *et al.* 2008, Khishe and Mosavi 2020, Mosavi *et al.* 2018, Khishe and Mosavi 2019, Mosavi *et al.* 2016, Mosavi *et al.* 2017). Non-parametric models, such as, a Bayesian framework for the Gaussian process regression (GPR) have recently received significant attention in the field of ML (Mahmoodzadeh *et al.* 2022). GPR provides a probabilistic, non-parametric modelling approach, and is being applied to various engineering problems. The use of GPR for modeling geotechnical or geological engineering problems is a relatively recent development. However, there is no research on the GPR for prediction of squeezing phenomenon along tunnel alignment.

In order to forecast the squeezing phenomenon along tunnel route, the GPR technique is utilized by this study. However, the key features of the GPR model which motivate us to use them, are as follows: 1) GPR directly captures the model uncertainty. As an example, in regression, GPR directly gives a distribution for the prediction value, rather than just one value as the prediction. This uncertainty is not directly captured in neural networks. 2) When using GPR, we are able to add prior knowledge and specifications about the shape of the model by selecting different kernel functions. For example, based on the answers to the following questions we may choose different priors. Is the model smooth? Is it sparse? Should it be able to change drastically? Should it be differentiable? This capability gives researchers flexible models, which can fit various kinds of datasets.

In order to train the GPR model, all input data are taken from the empirical, semi-empirical, and theoretical-analytical methods. To verify its feasibility, this technique as well as the other intelligence techniques is applied to Alborz service tunnel on Tehran–Shomal in Iran to predict squeezing phenomenon. One of the strengths of the proposed model is the data used to train it, in which various empirical, semi-empirical, and theoretical-analytical methods are used. This means that several different empirical, semi-empirical, and theoretical-analytical methods are considered in our proposed model at the same time. Also, since the input data of the trained model are obtained from only one tunnel (Alborz tunnel), it can reduce the comprehensiveness of the model for other tunneling projects. This can be one of the serious limitations of our proposed model.

2. Empirical, semi-empirical and theoretical-analytical methods of squeezing

The squeezing potential of weak rocks located on the tunnels route has been evaluated by various methods. The most important of these methods can be empirical methods, such as, Singh *et al.* (1992) and Goel *et al.* (1995), semi-empirical methods, such as, Aydan *et al.* (1993), Jethwa *et al.* (1984) and Hoek and Marinos (2000) and theoretical-analytical methods, such as International Society for Rock Mechanics (ISRM). Since in this study the above-mentioned methods have been used to estimate the squeezing condition and because of their use in learning the GPR model in the tunnel pathway, thus, in the following, a brief description of each of them will be presented.

2.1 Empirical methods

The empirical methods are based on the experience and comparison of different case histories. There are three categories of empirical approaches based on the indicators used:

1) Strength-stress ratio approach
2) Strain estimation approach
3) Rock mass classification approach

The tow Singh *et al.* (1992) and Goel *et al.* (1995) approaches are described in this section and has been used for the analysis in this article.

2.1.1 Singh et al. (1992) approach

This method of analysis is based on the rock mass classification approach. Singh *et al.* (1992) developed an empirical relationship from the log-log plot between the tunnel depth (H) and the logarithmic mean of the rock mass quality (Q) (See Fig. 1). 41 tunnel sections data were used to plot Fig. 1. Out of 41 data, 17 data were taken from case histories in Barton *et al.* (1974) and 24 tunnel section data were obtained from tunnels in Himalayan region. A clear line of demarcation can be seen on Fig. 1, which is in between the elastic and squeezing condition (Basnet 2005). The equation of this line is given as

$$H = 350\ Q^{1/3} \tag{1}$$

From Fig. 1, it can be concluded that the squeezing phenomenon may occur in the rock mass when depth of overburden above tunnel section exceeds $350\ Q^{1/3}$.

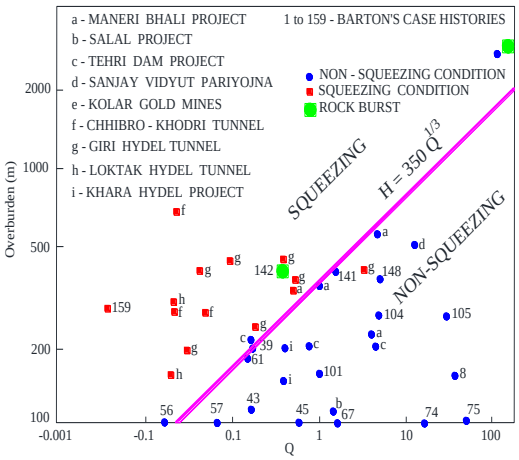

Fig. 1 Criteria for predicting squeezing ground.

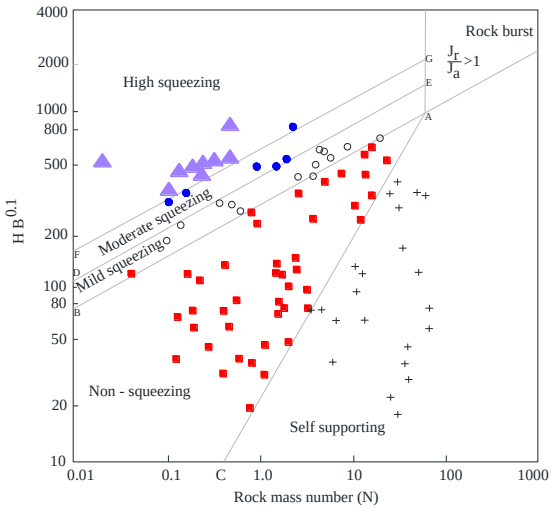

Fig. 2 Criteria for predicting squeezing ground (Goel *et al.* 1995)

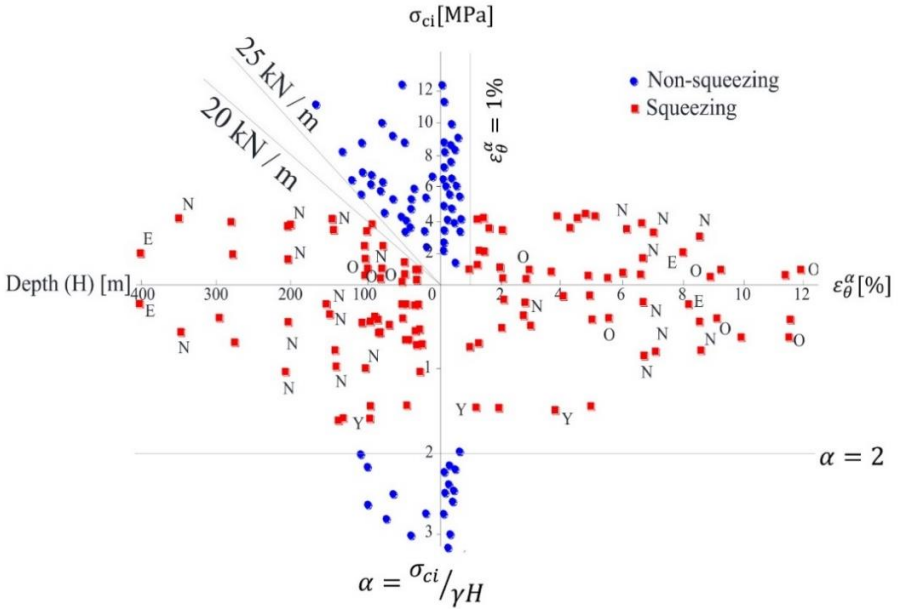

Fig. 3 Criteria for predicting squeezing ground (Aydan *et al.* 1993)

2.1.2 Goel et al. (1995) approach

A simple empirical approach developed by Goel *et al.* (1995) is based on the rock mass number N, defined as stress-free Q as follows.

$$N = Q_{SRF=1} \tag{2}$$

which is used to avoid the problems and uncertainties in obtaining the correct rating of parameter SRF in Barton *et al.* (1974) Q.

Goel *et al.* (1995) considered the tunnel depth H, the tunnel span or diameter B, and the rock mass number N of 99 tunnel sections. Out of 99 data, 39 data were taken from case histories in Barton *et al.* (1974) and 60 of them were obtained from projects in India. As shown in Fig. 2, Goel *et al.* (1995) have plotted the available data on a log-log diagram between N and $H \times B^{0.1}$. As shown in the same Fig. 2, a line demarcates the squeezing and non-squeezing cases. The equation of this line is

$$H = (275\ N^{0.33})B^{-0.1} \tag{3}$$

The top and bottom points of the line in the diagram, represent the conditions of the squeezing and non-squeezing properties, respectively. This can be summarized as follows:

for squeezing conditions

$$H \gg (275\ N^{0.33})B^{-0.1} \tag{4}$$

for non-squeezing conditions

$$H \ll (275\ N^{0.33})B^{-0.1} \tag{5}$$

2.2 Semi-empirical methods

The semi-empirical approaches that were used for the analysis of tunnel squeezing phenomenon are Aydan *et al.* (1993), Jethwa *et al.* (1984), Hoek and Marinos (2000), etc. These three methods are described in this section and has been used for the analysis in this article.

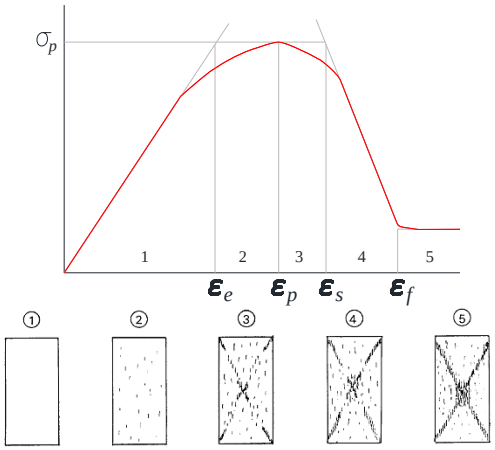

Fig. 4 Idealised stress-strain curve and associated states for squeezing rocks (Aydan *et al.* 1993)

Table 1 Classification of squeezing behaviour according to Aydan *et al.* (1993).

Class No.	Squeezing degree	Symbol	Theoretical expression	Comments on tunnel behaviour
1	Non-squeezing	NS	$\varepsilon_\theta^\alpha \,^*/_{\varepsilon_\theta^e} \leq 1$	The rock behaves elastically and the tunnel will be stable as the face ef-fect ceases
2	Light-squeezing	LS	$1 < {}^{\varepsilon_\theta^\alpha}/_{\varepsilon_\theta^e} < \eta_p$	The rock exhibits a strain-hardening be-haviour. As a result, the tunnel will be stable and the displacement will converge as the face effect ceases
3	Fair-squeezing	FS	$\eta_p < {}^{\varepsilon_\theta^\alpha}/_{\varepsilon_\theta^e} < \eta_s$	The rock exhibits a strain-softening be-haviour and the dis-placement will be larger. However, it will converge as the face ef-fect ceases
4	Heavy-squeezing	HS	$\eta_s < {}^{\varepsilon_\theta^\alpha}/_{\varepsilon_\theta^e} < \eta_f$	The rock exhibits a strain-softening at much higher rate. Subsequently, displacement will be larger and it will not tend to converge as the face effect ceases
5	Very heavy-squeezing	VHS	$\eta_f < {}^{\varepsilon_\theta^\alpha}/_{\varepsilon_\theta^e}$	The rock flows, which will result in the col-lapse of the medium and the displacement will be very large and it will be necessary to re-excavate the opening and install heavy sup-ports

*For η_p, η_s and η_f see Eq. (6); $\varepsilon_\theta^\alpha$: Tangential strain around a circular tunnel in a hydrostatic stress field (Aydan *et al.* 1993); ε_θ^e: Elastic strain limit for the rock mass

2.2.1 Aydan et al. (1993) approach

Aydan *et al.* (1993), based on the experience with tunnels in Japan, proposed to relate the strength of the intact rock σ_{ci} to the overburden pressure γH (γ is the rock mass unit weight and H is the tunnel depth below surface), by implying that the uniaxial compressive strength of the intact rock σ_{ci} and of the rock mass σ_{cm} are the same. As shown in Fig. 3, squeezing conditions will occur if the ratio $\sigma_c/\gamma H$ is less than 2.

The fundamental concept of the method is based on the analogy between the stress-strain response of rock in laboratory testing and tangential stress-strain response around tunnels. According to Fig. 4, five distinct modes occur during the loading time at low confining stress σ_3. The following relations are defined, which give the normalized strain levels η_p, η_s and η_f:

$$\eta_p = \frac{\varepsilon_p}{\varepsilon_e} = 2\sigma_{ci}^{-0.17},\ \eta s = \frac{\varepsilon_s}{\varepsilon_e} = 3\sigma_{ci}^{-0.25},\ \eta_f = \frac{\varepsilon_f}{\varepsilon_e} = 5\sigma_{ci}^{-0.32} \quad (6)$$

where ε_p, ε_s and ε_f are the strain values shown in Fig. 4, as ε_e is the elastic strain limit.

Based on a closed form of analytical solution, which has been developed for computing the strain level $\varepsilon_\theta^\alpha$ around a circular tunnel in a hydrostatic stress field, the five different degree of squeezing and some comments on the expected tunnel behaviour are defined as shown in Table 1.

2.2.2 Jethwa et al. (1984) approach

Jethwa *et al.* (1984), provided the degree of squeezing as follows

$$N_c = \frac{\sigma_{cm}}{p_0} = \frac{\sigma_{cm}}{\gamma\ H} \quad (7)$$

where, σ_{cm} is the rock mass uniaxial compressive strength, p_0 is the in situ stress, γ is the rock mass unit weight, and H is the tunnel depth below surface.

According to the Eq. (7), Jethwa *et al.* (1984) defined the squeezing condition for the four classes that are shown in Table 2.

2.2.3 Hoek and Marinos (2000) approach

Hoek (1998) used the ratio of the rock mass uniaxial compressive strength σ_{cm} to the in situ stress p_0 as an

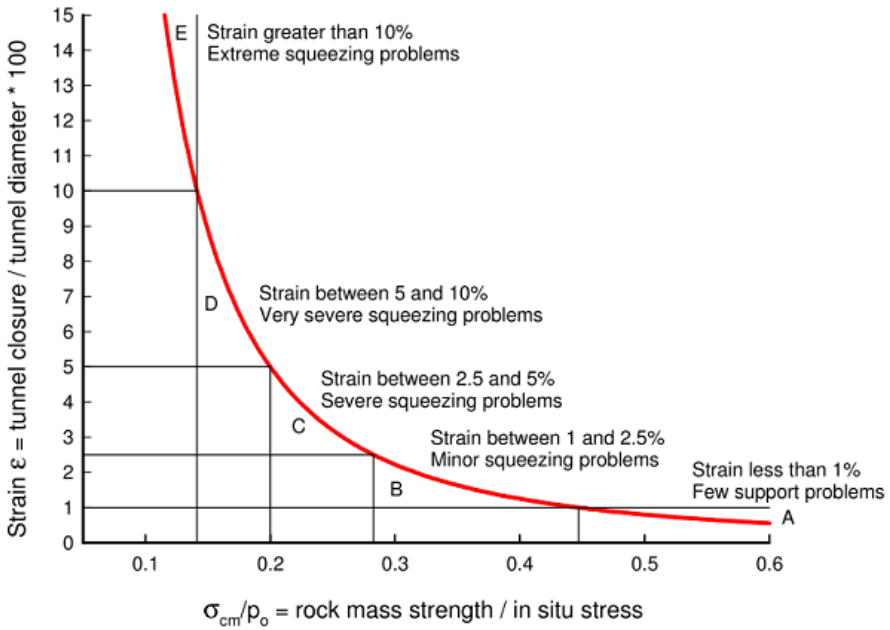

Fig. 5 Approximate relationship between strain and the degree of difficulty associated with tunneling through squeezing rock in case of unsupported tunnel in Hoek and Marinos (2000) approach (Basnet 2005)

Table 2 Classification of squeezing behaviour according to Jethwa *et al.* (1984).

σ_{cm}/p_0	Type of behaviour
< 0.4	Highly squeezing
0.4 – 0.8	Moderately squeezing
0.8 – 2	Mildly squeezing
> 2	Non-squeezing

indicator of potential tunnel squeezing problem. In particular, Hoek and Marinos (2000), by studying a number of tunnels in Venezuela, Taiwan, and India, showed that a plot of tunnel strain ε_t (defined as the percentage ratio of radial tunnel wall displacement to the tunnel radius) against the ratio σ_{cm}/p_0 can be used effectively to assess tunneling problems under squeezing condition (See Fig. 5). Hoek and Brown's criterion for estimating the strength and deformation characteristics of rock masses assumes that rock mass behaves isotropically. However, if the rock mass is heavily fractured, the continuity of the bedding surfaces will have been disrupted and the rock may behave as an isotropic mass. Thus, this criterion can be adapted also to weak heterogeneous rock masses (Fatemi Aghda *et al.* 2016).

Hoek (2000), in his recent 2000 Terzaghi lecture on "Big tunnels in bad rock", by means of axi-symmetric finite element analyses, and a range of different rock masses, in situ stresses and support pressures p_i gave the following approximate relationship (Eq. (8)) for the tunnel strain ε_t.

$$\varepsilon_t(\%) = 0.15(1 - p_i/p_0)\frac{\sigma_{cm}^{-(3p_i/p_0+1)/(3.8p_i/p_0+0.54)}}{p_0} \quad (8)$$

According to Eq. (8), squeezing does not occur unless tunnel strain is greater than 1%. Based on field observations and measurements, Sakurai (1983) suggested that tunnel strain levels exceeding approximately 1% are associated with the onset of tunnel instability and involve in difficulties in providing adequate support. The 1% limit proposed by Sakurai is only an indication of the need for further support and it should not be assumed that sufficient support is not installed in the tunnel. In fact, in some cases, it is desirable to allow the tunnel to undergo strains of as much as 5% before activating the support (Fatemi Aghda *et al.* 2016).

Hoek and Marinos (2000) also suggested the classifications of squeezing severity based on the strain percentage. There are five classes of squeezing problems from few support problems to extreme squeezing problems i.e.; from A to E. The ranges of these classes and their description are shown in Fig. 5 and Table 3 (Basnet 2005).

2.3 Theoretical- analytical methods

Theoretically, the squeezing condition around a tunnel opening is encountered when tangential stress is bigger than rock strength. Barton *et al.* (1974) suggested that the ratio of maximum tangential stress (calculated from elastic theory) to unconfined compression strength ($\sigma_\theta/\sigma'_\theta$) can be used to define squeezing rock pressure. Singh *et al.* (1992) suggested that a necessary condition for squeezing rock conditions is (Fatemi Aghda *et al.* 2016)

$$\sigma_\theta > q_c \quad (9)$$

where σ_θ is the tangential stress and q_c is the uniaxial crushing strength of the rock mass.

Theoretical-Analytical methods such as International Society for Rock Mechanics (ISRM), are based on the analytical methods of the closed form. In these methods, the squeezing potential is divided into four classes according to Table 4.

Table 3 Squeezing classes and appropriate support types (Hoek and Marinos 2000)

	Strain ε (%)	Geotechnical issues	Support types
A	<1	Few stability problems and very simple tunnel support design methods can be used. Tunnel support recommendations based upon rock mass classification provide an adequate basis for design.	Very simple tunneling condition, with rockbolts and shotcrete typically used for support.
B	1 – 2.5	Convergence confinement methods are used to predict theformation of a plastic zone in the rock mass surroundinga tunnel and of the interaction between the progressive development of this zone and different types of support.	Minor squeezing problems, which are generally dealt with by rockbolts and shotcrete; sometimes with light steel sets or lattice girders, are added for additional security.
C	2.5 – 5	Two-dimensional finite element analysis, incorporating support elements and excavation sequence are normally used for this type of problem. Face stability is generally not a major problem.	Severe squeezing problems requiring rapid installation of support and careful control of construction quality. Heavy steel sets embedded in shotcrete are generally required.
D	5 – 10	Face stability issues dominate the design of the tunnel. While two-dimensional finite analyses are generally carried out, some estimates of the effects of forepoling and face reinforcement are required.	Very severe squeezing and face stability problems. Forepoling and face reinforcement with steel sets embedded in shotcrete are usually necessary.
E	>10	Severe face instability as well as squeezing of the tunnel make this an extremely difficult three-dimensional problem for which no effective design methods are currently available. Most solutions are based on experience	Extreme squeezing problems. Forepoling andface reinforcement are usually applied and yielding support may be required in extreme cases.

Table 4 Segmentation of squeezing conditions into four classes in ISRM methods

ISRM	Squeezing condition
$\sigma_\theta/\sigma_{cm} < 1$	Non-squeezing
$1 \le \sigma_\theta/\sigma_{cm} \le 2$	Low squeezing
$2 \le \sigma_\theta/\sigma_{cm} \le 4$	Moderate squeezing
$\sigma_\theta/\sigma_{cm} \ge 4$	High squeezing

*σ_{cm}: Rock mass uniaxial compressive; p_0: Uniaxial crushing strength of the rock mass; σ_θ: Tangential stress of the rock mass

3. Gaussian process regression

Despite the merits of various Machine Learning (ML) approaches, according to the No-Free-Lunch (NFL) theorem, there is no ML model to solve all engineering problems as the best method successfully. Therefore, researchers have tried to evaluate the efficiency of various ML approaches for solving various optimization. We use six ML models with different features and capabilities as an NFL theorem, including GPR, SVR, DT, and LR. However, the key features of the models as mentioned earlier, which motivate us to use them, are as follows:

- **Regression Analysis**

Regression analysis predicts a continuous target variable from one or multiple independent variables. Typically, regression analysis is used with naturally-occurring variables rather than variables that have been manipulated through experimentation. As stated above, there are many different types of regression, so once we've decided regression analysis should be used, how do we choose which regression technique should be applied?

- **GPR**
  - GPR directly captures the model uncertainty. As an example, in regression, GPR directly gives you a distribution for the prediction value, rather than just one value as the prediction. This uncertainty is not directly captured in neural networks.
  - When using GPR, you are able to add prior knowledge and specifications about the shape of the model by selecting different kernel functions. For example, based on the answers to the following questions you may choose different priors. Is the model smooth? Is it sparse? Should it be able to change drastically? Should it be differentiable? This capability gives researchers flexible models, which can fit various kinds of datasets.

GPR models are based on the assumption that adjacent observations should convey information about each other. GPs are a way of specifying a prior directly over function space. This is a natural generalization of the Gaussian distribution, whose mean and covariance are a vector and matrix, respectively. The Gaussian distribution is over vectors, whereas the Gaussian process is over functions. Thus, due to prior knowledge about the data and functional dependencies, no validation process is required for generalization and GPR models are able to understand the predictive distribution corresponding to the test input (Pal and Deswal 2010).

Probabilistic regression is usually formulated as follows: given a training set $\mathcal{D} = \{(x_i, y_i), i = 1, \ldots, n\}$ of n pairs of (vectorial) inputs x_i and noisy (real, scalar) outputs y_i, compute the predictive distribution of the function values f^* (or noisy y^*) at test locations x^*. In the simplest case (which we deal with here), we assume that the noise is additive, independent, and Gaussian, such that the relationship between the (latent) function $f(x)$ and the observed noisy targets y is given by (Quinonero-Candela and Rasmussen 2005)

$$y = f(x) + \epsilon \quad , \quad \epsilon \sim N(0, \sigma^2) \tag{10}$$

where, $f(x)$ represents an arbitrary regression function, while ϵ is the noise follows an independent, identically

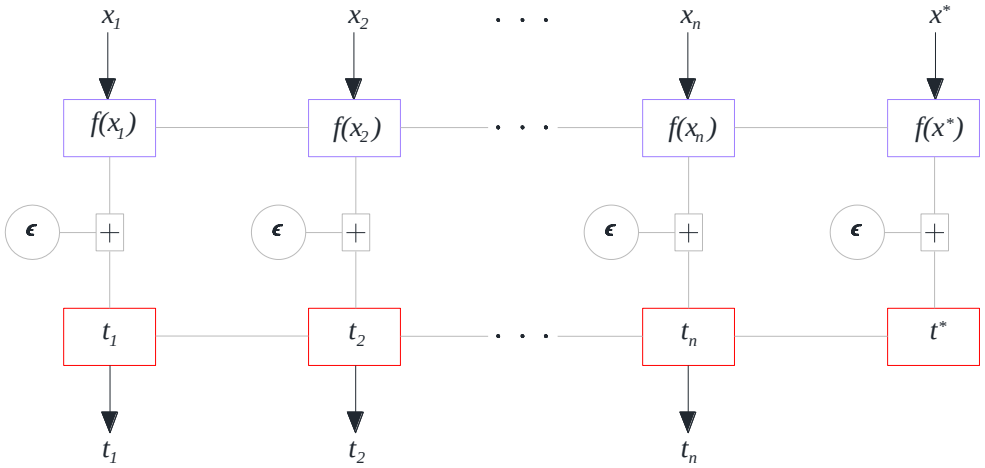

Fig. 6 Graphical model for GP (Quinonero-Candela and Rasmussen 2005)

distributed Gaussian distribution with zero mean (usually, for notational simplicity we will take the mean function to be zero and the offsets and simple trends can be subtracted out before modeling) and variance of the noise σ^2. The symbol ~ in statistics means sampling for.

A Gaussian process $f(x)$ can be represented as: $f(x) \sim \mathcal{GP}(m(x),k(x, x'))$, where $m(x)$ is the mean and $k(x, x')$ is the covariance (or kernel) function evaluated at x and x'. Furthermore, we assume that $f = [f(x_1), f(x_2), ..., f(x_n)]^T$ behaves according to a Gaussian process, that is $P(f \mid X = N(0,K))$, where K is the covariance matrix with element $K_{ij} = k(x_i,x_j)$ (Li *et al.* 2017, Kang *et al.* 2015).

$$K(X,X) = \begin{bmatrix} k(x_1,x_1) & k(x_1,x_2) & \cdots & k(x_1,x_n) \\ k(x_2,x_1) & k(x_2,x_2) & \cdots & k(x_2,x_n) \\ \vdots & & \vdots \; \vdots & \vdots \\ k(x_n,x_1) & k(x_n,x_2) & \cdots & k(x_n,x_n) \end{bmatrix} \quad (11)$$

The element K_{ij} is the covariance between values of the latent functions $f(x_i)$ and $f(x_j)$, and it encodes about the prior of our knowledge of nonlinear process among latent functions.

GPR is used to compute the predictive distribution of the function values f^* at test points $X^* = [x_1^*, x_2^*, ..., x_m^*]$ (Yuan *et al.* 2008, Li *et al.* 2017, Kang *et al.* 2015). A graphical model representation of a GP is given in Fig. 6 (circled variables are random variables and non-circled ones are observed/given). In the figure, for given $\{x_1, x_2, ..., x_n, x^*\}$, the corresponding set of random variables $\{f(x_1), f(x_2), ..., f(x_n), f(x^*)\}$ have a joint multivariate Gaussian distribution. With the additive independent white noise assumption, the corresponding circled $\{t_1, t_2, ..., t_n, t^*\}$ are also jointly normally distributed. The marginal part of the joint gives us the probability of the data $\{t_1, t_2, ..., t_n\}$ and the posterior predictive distribution of $f(x^*)$ (or equivalently t^*) corresponding to x^* is obtained by conditioning on the data and x^* (Quinonero-Candela and Rasmussen 2005).

Now, suppose we have collected observations $\mathcal{D}_t = \{X_t,y_t\}$ and we want to make predictions for new inputs X^* by drawing f^* from the posterior distribution $p(f|\mathcal{D}_t)$. By definition, previous observations y_t and function values f^* follow a joint (multivariate) normal distribution. This distribution can be written as (Schulz *et al.* 2018)

$$\begin{bmatrix} y_t \\ f^* \end{bmatrix} \sim N\left(0, \begin{bmatrix} K(X_t,X_t) + \sigma_\epsilon^2 I & K(X_t,X^*) \\ K(X^*,X_t) & K(X^*,X^*) \end{bmatrix}\right) \quad (12)$$

where I is an identity matrix (with 1's on the diagonal and zero elsewhere) and σ_ϵ^2 is the assumed noise level of observations (i.e., the variance of ϵ) (Schulz *et al.* 2018). Deriving the conditional distribution corresponding to $f(x) \sim \mathcal{GP}(m(x),k(x,x'))$, we arrive at predictive distribution, the key predictive equations for GPR are Eqs. (13) and (14).

The output estimates are made not only with an expected prediction (mean) of latent function f^*, but also with a measure of uncertainty (variance) (Yuan *et al.* 2008, Li *et al.* 2017, Schulz *et al.* 2018).

$$\bar{f}^* = K(X^*,X)[K(X,X) + \sigma^2 I]^{-1} y \quad (13)$$

$$cov(f^*) = K(X^*,X^*) - K(X^*,X)[K(X,X) + \sigma^2 I]^{-1} K(X,X^*) \quad (14)$$

The most commonly used squared exponential covariance function with automatic relevance determination distance measure was adopted (Kang *et al.* 2015) (See Eq. (15)).

$$k(x_p,x_q) = \sigma_f^2 exp\left(-\frac{1}{2}(x_p - x_q)^T M (x_p - x_q)\right) = \sigma_f^2 exp\left(-\frac{1}{2}\sum_{i=1}^{D}\frac{(x_{p,i} - x_{q,i})^2}{l_i^2}\right) \quad (15)$$

where $M = diag(l)^{-2}$, $l = [l_1, l_2, ..., l_D]^T$. $\theta = (\ln l_1, ..., \ln l_D, \ln \sigma_f)$ are the hyper-parameters.

The kernel normally contains hyper-parameters, such as, the length-scale, the signal variance, and the noise variance. These are usually not assumed to be known, but rather are learned from the data. As the posterior distribution over the hyper-parameters is generally difficult to obtain, full Bayesian inference of the hyper-parameters is generally not used. Instead, a point estimate of the hyper-parameters is usually computed by maximizing the log-marginal likelihood. This is similar to parameter estimation by

maximum likelihood and is referred to as type-II maximum likelihood (Schulz *et al.* 2018).

Given the data $S = \{X,y\}$ and hyper-parameters θ, the log-marginal likelihood is

$$\log p(y|X,\theta) = -\frac{1}{2}y^T(K_y)^{-1}y - \frac{1}{2}log|K_y| - \frac{n}{2}log2\pi \quad (16)$$

where $K_y = K(X,X) + \sigma_\epsilon^2 I$ is the covariance matrix of the noisy output values y. The log-marginal likelihood can be viewed as a penalized t measure, where the term $-1/2\, y^T K_y^{-1} y$ measures the data fit, that is how well the current kernel parametrization explains the dependent variable, and $-1/2\, log|K_y|$ is a complexity penalization term. The final term $-n/2\, log2\pi$ is a normalization constant (Schulz *et al.* 2018).

4. Engineering application

To verify the described methods in sections 2 and 3, they are applied to Alborz service tunnel on Tehran–Shomal motorway project in Iran to predict the squeezing condition along tunnel route. The experiment is described in the following subsections in detail.

4.1 Engineering background

The Tehran-Shomal motorway project in Iran is a new motorway to connect the capital Tehran with the city of Chalus at the Caspian Sea in the North. The total length is 121 km. Currently traffic runs on small roads passing the Alborz mountains and the journey takes five to six hours. Upon completion of the project the travelling time will reduce to less than two hours with an overall higher capacity. The motorway alignment has more than 30 twin tunnels for double lanes. The Alborz tunnel will be the longest of these with a length of 6,400 *m* at an altitude of 2,400 *m* (Fig. 7) (Wenner and Wannenmacher 2008).

The service tunnel is located between the main tunnel tubes and is used for site investigation, drainage, and as access for the main tunnel construction. Currently, the service tunnel drilling is completed by the TBM, and now the main tunnels are excavated in a controlled firearm with a horseshoe cross section in two stages of the head and the bench. The entrance of the tunnel is considered the northen mouth (to the Shomal-S) and its outlet is considered the southern mouth (to the Tehran-T). The Lithology of the tunnel route is mainly composed of Tuffs, Andesite, Anidrite, Limestone, and Sandstone. The compressive strength of the rocks of the tunnel route varies from 20 to 120 MPa. The longest fault is located in the ST5339-5361 where the water flow into the tunnel is high from this fault and provides conditions for squeezing the rocks of the tunnel pathway.

The squeezing phenomenon occurred durring excavating of the tunnel at three different distances (ST3007-3015, ST3410-3424 and ST5339-5361), so that in the ST3007-3015, caused the TBM to be stopped for 12 days.

In this paper, the southern section of the Alborz service tunnel from ST2500 to ST6000 is used to predict squeezing conditions. In Fig. 8, the geological profile of the Alborz tunnel has been given. After construction of the Alborz service tunnel, all required data for empirical, semi-empirical and theoretical-analytical methods of squeezing forecasting were available. In the following sections, while investigating the squeezing phenomenon with each of the methods, this data will be provided

4.2 Empirical, semi-empirical, and theoretical-analytical methods of squeezing forecasting in the Alborz service tunnel

The studied section (ST3007-6000) is divided into 33 different regions according to geological conditions and the squeezing potential in each region is obtained by the empirical methods (Singh *et al.* 1992, Goel *et al.* 1995), the semi-empirical methods (Aydan *et al.* 1993, Jethwa *et al.* 1984, Hoek and Marinos 2000), and the theoretical-analytical methods (ISRM). In Fig. 9, the values obtained for each method, according to the number of squeezing classes (see section 2) and the weight of the obtained values, the squeezing potential for each method is expressed probabilistically.

According to the data obtained during the Alborz service tunnel construction, the squeezing phenomenon was occurred in regions 14, 20 and 31. In these regions we consider the squeezing potential equal to 100%. However, in other regions where the squeezing has not yet occurred, its potential is considered equal to zero. According to Fig. 9, in situations where the squeezing phenomenon actually occurred, the occurrence probability of squeezing obtained by Singh *et al.* (1992), Goel *et al.* (1995), and Aydan *et al.* (1993) methods is more than 70%. Therefore, it can be said that in these situations, these three methods have provided a good accuracy. However, the occurrence probability of squeezing in other situations by Singh *et al.* (1992) and Goel *et al.* (1995) methods is also high. This shows that Singh *et al.* (1992) and Goel *et al.* (1995) methods are conservative, which increase the cost of constructing the tunnel. Jethwa *et al.* (1984) method has a high probability of 40% for the occurrence of squeezing in positions 14, 20 and 31. The occurrence probability of squeezing in these situations for other methods is less than 40%. Therefore, it can be said here that Aydan *et al.* (1993) method offers better performance in the estimation of squeezing phenomenon.

4.3 GPR model of Alborz service tunnel

In the previous section, the potential of squeezing was estimated probabilistically by several different methods. In many situations in the Alborz service tunnel route, different methods provided different results. We must consider the best and most accurate method among the empirical, semi-empirical and theoretical-analytical methods and consider the GPR inputs based on it. Analyzing the diagram in Fig. 9, it was concluded that Aydan *et al.* (1993) method was more accurate in estimating the squeezing phenomenon. Therefore, in this study, 300 data were used to train the GPR model and 33 data for test, whose inputs and outputs

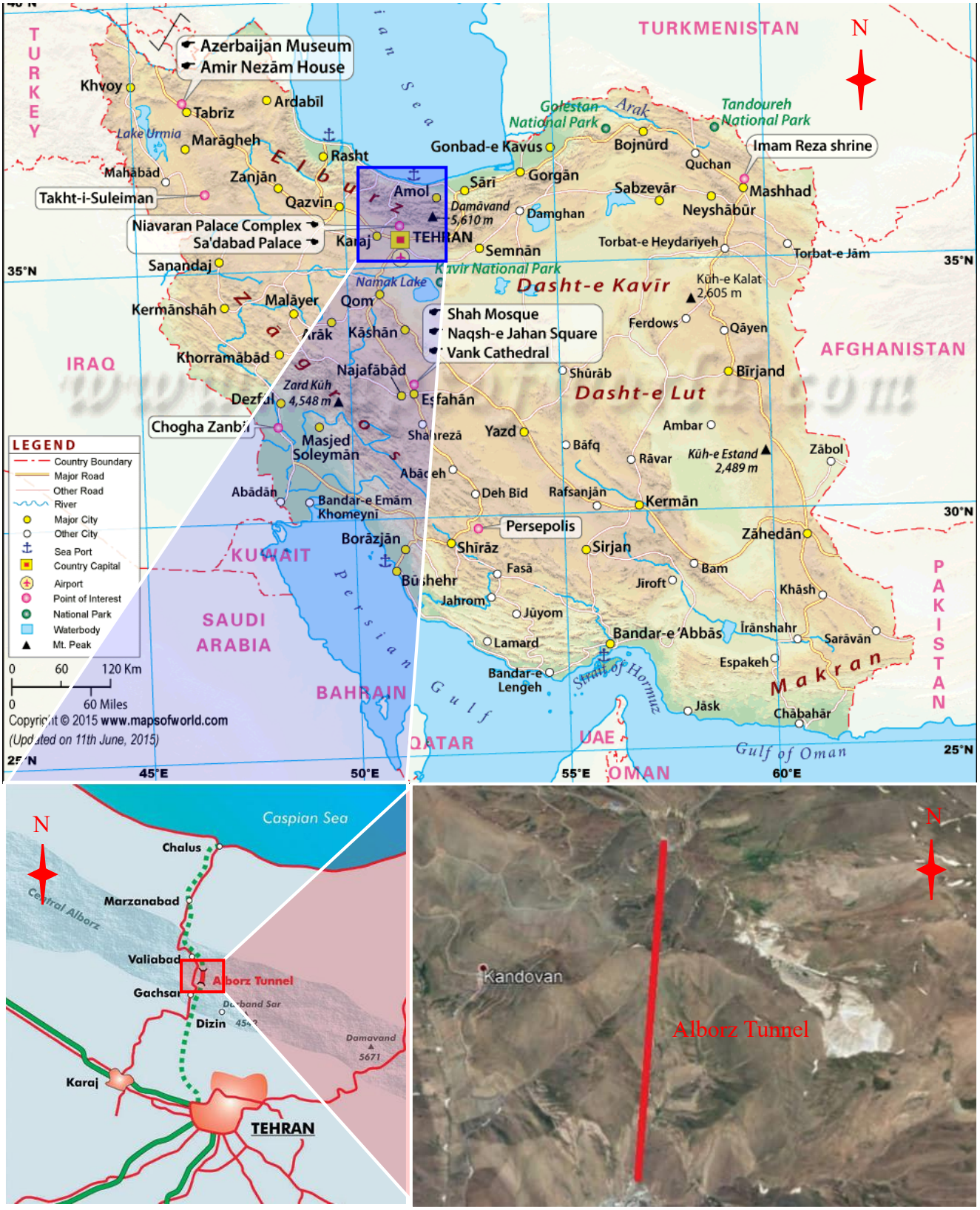

Fig. 7 Project location of the Alborz tunnel

were determined based on Aydan *et al.* (1993) method. A summary of the data used is given in Table 5.

After training the GPR model, the squeezing potential was presented (See Fig. 10), for the studied section of the Alborz service tunnel. Afterwards, the two SVR and ANN techniques were used to predict the squeezing conditions (See Fig. 10).

Concerning the parameter setting, in the GPR case, we

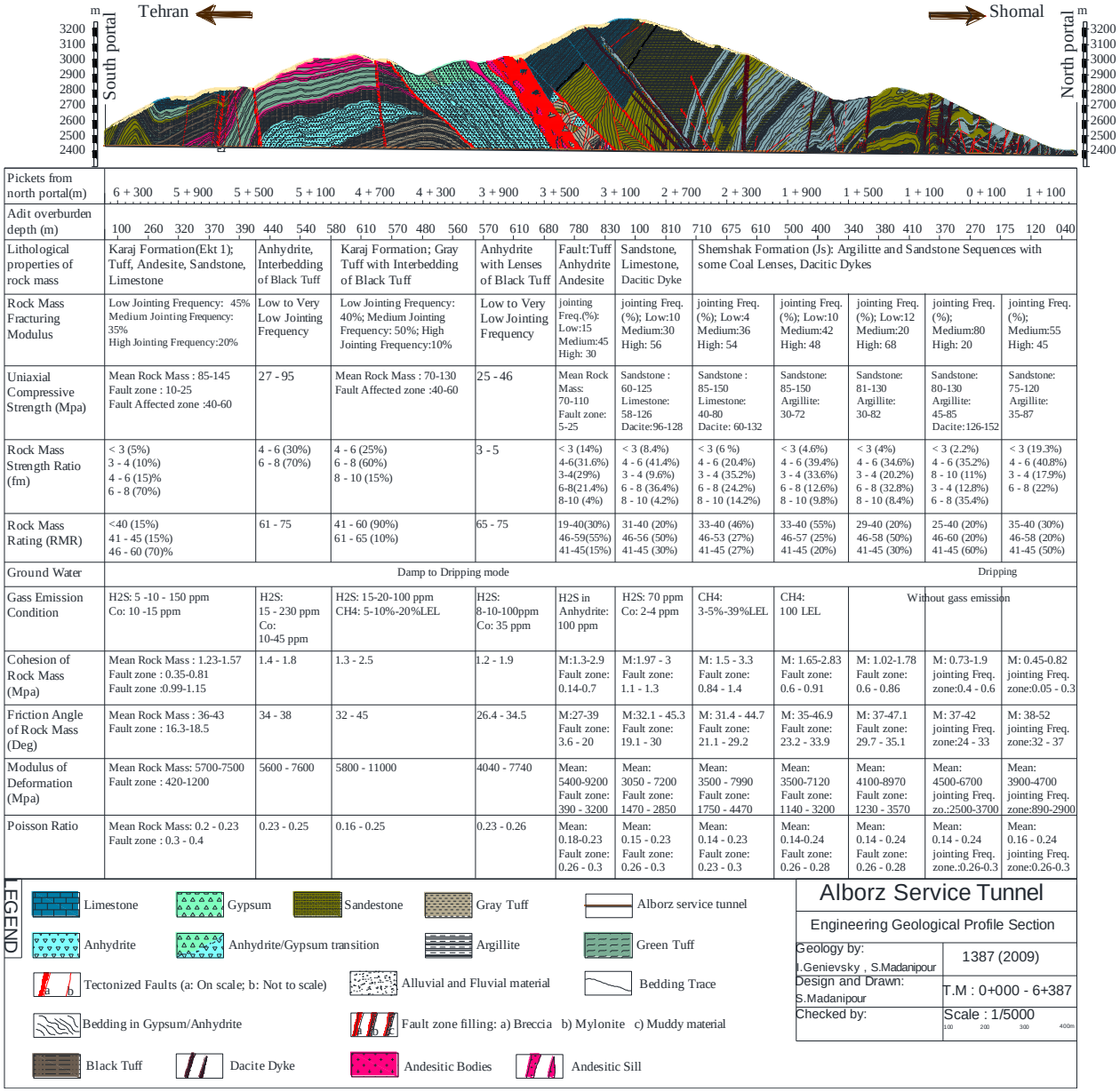

Fig. 8 Geological map of Alborz service tunnel

considered a squared exponential covariance function as it is presented in (Eq. (17). The kernel is very simple; it takes only two parameters: the length between the points and the average distance of them with the mean. We supposed to have a zero mean vector, so our distribution is around zero. Likewise, to match a signal with noise, we calculate their covariances as explained in Eq. (17). We can identify the high correlations through the nearby points, leading to high covariances. On the other hand, while using the squared exponential, it is impossible to extrapolate more than ℓ units between any two points.

$$k(x_p, x_q) = \sigma_f^2 exp\left(-\frac{1}{2}(x_p - x_q)^T \; M(x_p - x_q)\right) = \sigma_f^2 exp\left(-\frac{1}{2}\sum_{i=1}^{D}\frac{(x_{p,i} - x_{q,i})^2}{l_i^2}\right) \quad (17)$$

where $M = diag(l)^{-2}$, $l = [l_1, l_2, \dots, l_D]^T$ $\theta = (\ln l_1, \ln l_2, \dots, \ln l_D, \ln \sigma_f]^T$ are the hyper-parameters.

The kernel typically contains hyper-parameters such as length-scale, signal variance, and noise variance. These are usually assumed to be unknown but rather are trained from the data. Hence, generally, the posterior distribution over the hyper-parameters is difficult to be obtained, the full Bayesian inference of the hyperparameters usually is not used. As an alternative, a point estimate of the hyperparameters is generally computed by maximizing the log-marginal likelihood. This is similar to the parameter estimation by maximum likelihood and is referred to as type-II maximum likelihood. Here, we tuned the hyperactive parameters using the automatic hyperactive parameter optimization method given in MATLAB 2018 with the 'fitrgp' function in which the five-fold cross-validation loss is minimized.

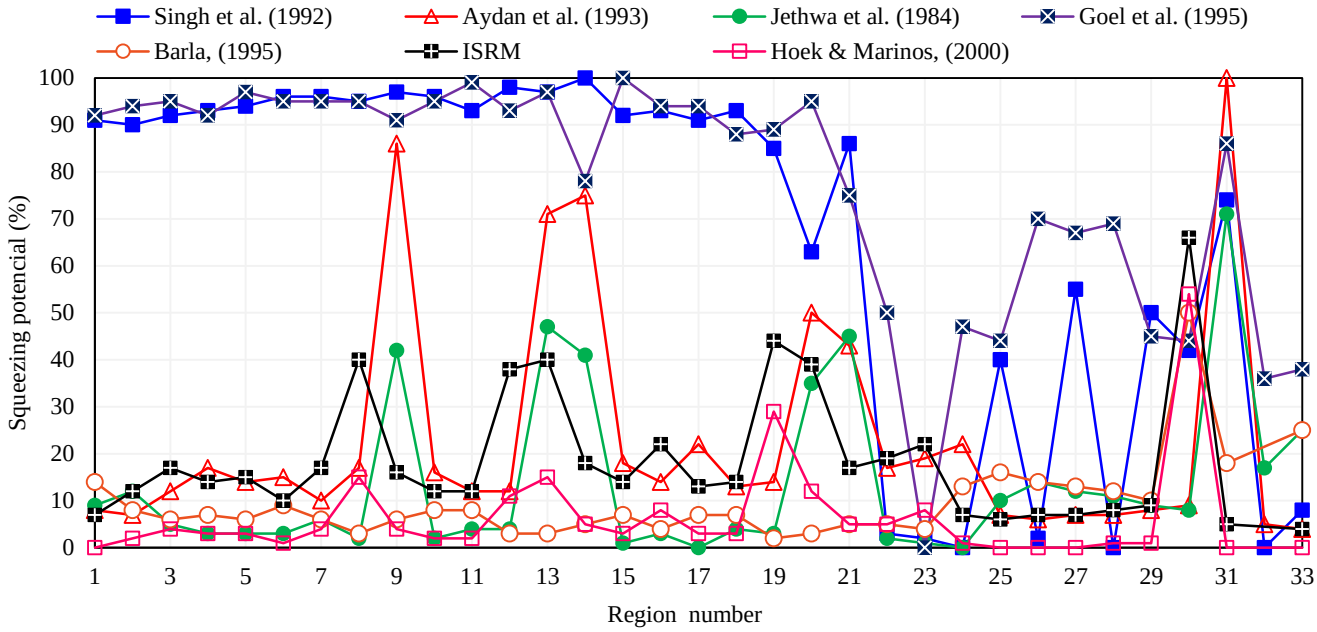

Fig. 9 The squeezing potential along Alborz service tunnel for the empirical, semi-empirical and theoretical-analytical methods considered in this study

Table 5 An overview on the database

Data		σ_{ci}^{*}	σ_{cm}	γH	η_p	η_s	η_f	$\varepsilon_\theta^\alpha$	ε_θ^e	OP [%]
Testing	count	33	33	33	33	33	33	33	33	33
	mean	62.70	35.61	17.81	1.02	1.12	1.43	5.86	9.94	22.94
	std	30.96	7.82	3.91	0.12	0.20	0.34	4.33	6.18	24.89
	min	8	16.82	8.41	0.87	0.89	1.06	0.60	0.82	4
	25%	37	30.07	15.03	0.93	0.98	1.20	2.63	5.72	8
	50%	65	38.07	19.03	0.98	1.05	1.31	5.66	10.14	14
	75%	85	42.48	21.24	1.08	1.21	1.57	6.81	12.50	19
	max	127	44.14	22.07	1.40	1.78	2.57	19.70	24.25	100
Training	count	300	300	300	300	300	300	300	300	300
	mean	83.56	45.81	34.27	1.85	1.50	2.13	11.50	8.50	15.31
	std	43.26	11.69	9.57	0.28	0.29	0.58	8.42	7.31	18.59
	min	8	4.72	4.05	0.41	0.53	0.81	0.60	0.63	1
	25%	46	50.17	20.55	0.83	0.70	1.02	3.20	6.30	9
	50%	79	61.28	33.26	1.13	1.26	1.37	7.04	12.56	17
	75%	93	65.37	38.42	1.39	2.52	1.78	10.35	15.82	24
	max	159	79.40	55.71	2.35	2.84	3.88	42.38	35.21	100
Input/Output		Input	Input	Input	Input	Input	Input	Input	Input	Output

*σ_{ci}: Uniaxial compressive strength of the intact rock; σ_{cm}: Uniaxial compressive strength of the rock mass; γ: Rock mass unit weight; H: Tunnel depth below surface; η_p,η_s and η_f: Normalized strain levels; $\varepsilon_\theta^\alpha$: Tangential strain and ε_θ^e is the elastic strain limit for the rock mass; OP: Occurrence probability

In the MATLAB software, four model types of rational quadratic, squared exponential, Matern 5/2, and exponential are exist for the GPR method. That model type, which presented the most accurate predictions, is considered as the GPR predictions. Here, the model type of Matern 5/2 was the most accurate one. The other parameters considered in the GPR model through the MATLAB software's optimization mode are presented in Table 6.

A Gaussian kernel for the SVR method is adopted. This choice is motivated by the excellent prediction accuracy and the limited computational complexity associated with this kernel. The regularization and kernel width parameters were

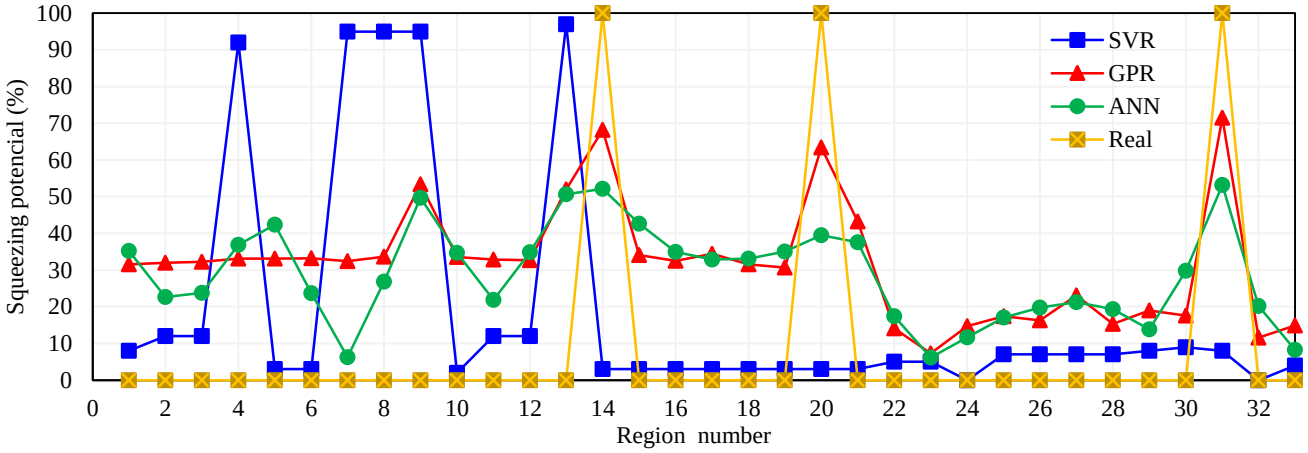

Fig. 10 Comparison GPR, SVR and ANN results with the actual squeezing potential along Alborz service tunnel

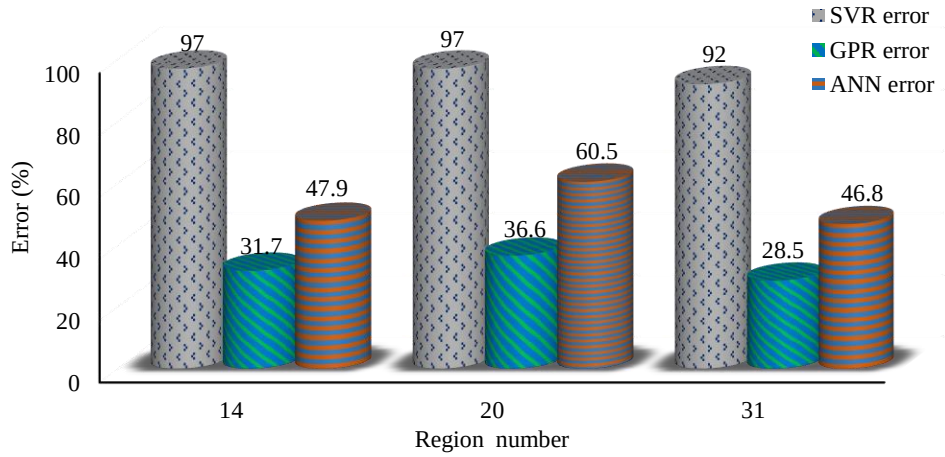

Fig. 11 The pridective percentage errors of the GPR, SVR and ANN methods in the three regions of 14, 20 and 31

Table 6 Optimized hyper-parameters of the GPR model

Parameter	Value or type
KernelFunction (Form of the covariance function)	'Matern 5/2'
BasisFunction (Explicit basis in the GPR model)	'Constant'
Beta (Initial value of the coefficients for the explicit basis)	5.74223e+01
Sigma (Initial value for the noise standard deviation of the Gaussian process model)	0.90568
FitMethod (Method to estimate parameters of the GPR model)	Exact Gaussian process regression

Table 7 Optimized hyper-parameters of the SVR model

Parameter	Value or type
Kernel Function	'Gaussian'
Epsilon (Half the width of epsilon-insensitive band)	1.1119
Solver (Optimization routine)	'SMO'
Bias	27.0086
Mu	658.5426
Sigma	444.3355

tuned using the automatic hyperactive parameter optimization method given in MATLAB 2018 with the 'fitsvr' function. Six types of SVR models, including linear, quadratic, cubic, fine Gaussian, medium Gaussian, and coarse Gaussian, are applied in the SVR model. All of these models made the squeezing predictions, and the best one was considered. The best model types and hyper-parameter values for the SVR method are given in Table 7.

For the ANN, the convolutional forward backpropagation algorithm with the Levenberg–Marquardt technique is utilized. Besides, we set up a three-layer network with one neuron in the input layer, 15 neurons in the hidden layer, and one neuron in the output layer.

According to the available information after construction of the Alborz service tunnel, during construction, in three regions of 14, 20 and 31, the squeezing phenomenon has occurred and for a few days, this has created problems for the TBM. In these points we consider the squeezing potential to be 100%. However, in other situations where squeezing has not yet occurred and

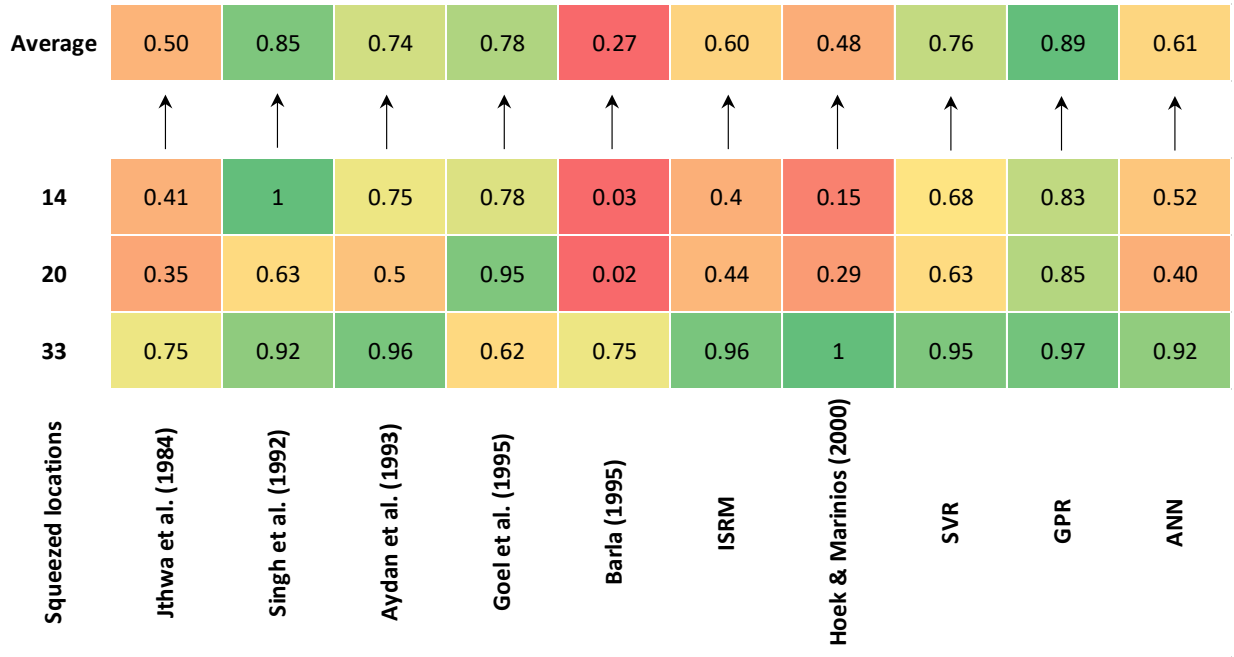

Fig. 12 Results comparison in the three regions of 14, 20 and 31 using the accuracy matrix

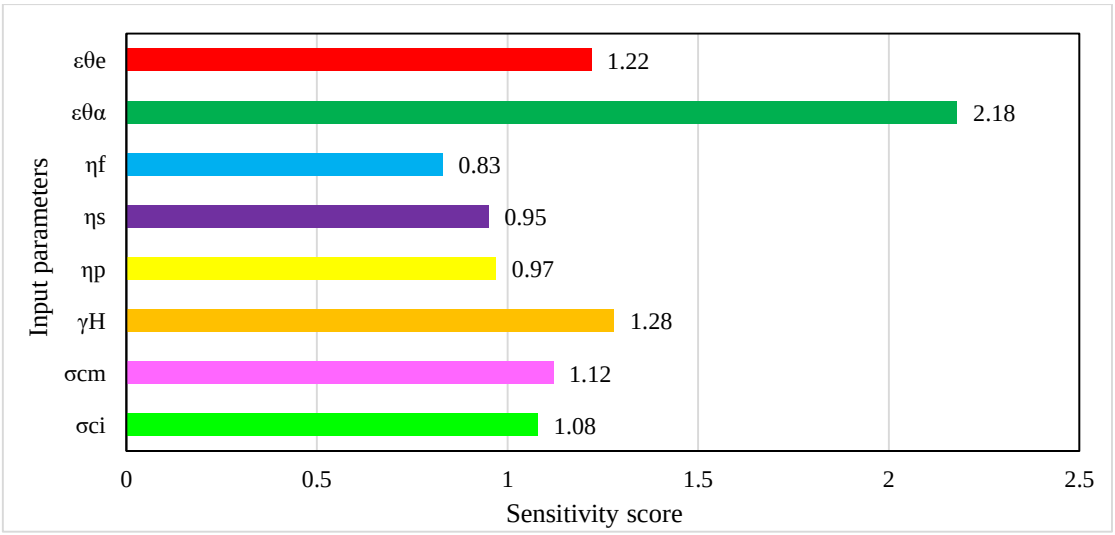

Fig. 13 Sensitivity score of the input parameters on the prediction of squeezing phenomenon using MIT method

its amount is considered zero. If we want to compare the error of each of the three methods with the real state as shown in Fig. 11, we find that the results of the GPR and ANN are closer together. In general, the GPR has less error and approximates predictions with good probability in the situations that have actually been squeezed. Nevertheless, the SVR predictions are less accurate than GPR and ANN. Thus, these data can be used to build the main tunnels that are currently being excavated, and in areas where squeezing potential is more likely to be predicted, be cautious and take the necessary measures.

5. Discussion

Here we want to made a comparative analysis between existing conventional methods and ML methods. In Fig. 12, to comprehensively evaluate the models' performance, the occurrence probability of the squeezing phenomenon estimated using the empirical, semi-empirical, theoretical-analytical, and ML methods are displayed through a recently proposed thermal map matrix called the accuracy matrix. Considering the ideal value as a reference, the accuracy obtained by the developed models is calculated. In the locations 14, 20, and 31, the occurrence probability of squeezing phenomenon was considered equal to 100%. Therefore, the ideal value for the squeezing occurrence in these locations is considered equal to 100%. Fig. 12 shows the accuracy of predictions in positions 14, 20 and 31 for each model. The average accuracy for each model is also shown. As it turns out, the GPR method with the average accuracy of 0.89 has the highest prediction accuracy. Singh

et al. (1992) and Goel *et al.* (1995) methods also showed good performance with average accuracy of 0.85 and 0.78, respectively. But, as mentioned earlier, given the Singh *et al.* (1992) and Goel *et al.* (1995) methods in Fig. 9, in other situations where squeezing has not occurred, the occurrence probability is high. These methods are very conservative and designing based on these methods can significantly increases the construction costs. The SVR and Aydan *et al.* (1993) methods with accuracies of 0.76 and 0.74, respectively, have provided a good ability to estimate the occurrence of squeezing. The lowest accuracy is provided by the Barla (1995) method, which is equal to 0.27. So, these results showed us that the GPR model can provide a better performance in predicting the squeezing phenomenon than other methods considered in this paper.

An issue that is very important in the ML methods is the type of model input parameters. It is better to consider parameters as the model inputs that have a great impact on the model output. Sometimes considering too many parameters as the model inputs can lead to overfitting and model malfunction. Therefore, in the ML methods, it is necessary to determine the most effective parameters on the output and apply them as the model's inputs. In this article, the mutual information test (MIT) is used to detect the sensitivity of the input parameters individually on the squeezing phenomenon. The MIT is a filtering technique applied to capture the desired relationship between each parameter and the label. This measure is the interdependence between parameters and shows the strength of the relationship between them. The information gain can calculate the mutual information size between the parameters

$$Gain(Y,X) = Ent(Y) - \sum_{v=1}^{V} \frac{|Y^v|}{|Y|} Ent(Y^v) \qquad (18)$$

where v indicates the number of all possible values for X, Y^v is the set Y related to when x takes x_v, and Ent(Y) is the entropy of the information. As $Gain(Y,X)$ increases, the correlation between X and Y is increased.

Lastly, according to the score of the parameters in the MIT method, the importance degree of the input parameters on the squeezing phenomenon was calculated. The results obtained by the MIT method are illustrated in Fig. 13 for each input parameter. Looking at Fig. 13, the most sensitive parameter on the squeezing phenomenon is the $\varepsilon_\theta^\alpha$ with a sensitivity score of 2.18. Parameter η_f has the least impact on the squeezing. The sensitivity score for the η_f, η_s, and η_p are less than 1. Therefore, to avoid the complexity of the model and the overfitting problem, we can ignore these parameters and only consider five parameters of σ_{ci}, σ_{cm}, γH, $\varepsilon_\theta^\alpha$ and ε_θ^e as the model's inputs. Considering only these five parameters in our ML models, caused the average accuracy provided by the GPR, SVR and ANN methods to increase to 0.92, 0.84 and 0.73, respectively.

6. Conclusions

Squeezing is one of the most important issues that must be considered before building subsurface projects in weak rocks. Due to the unknown subsurface conditions before construction, various empirical, semi-empirical and theoretical-analytical methods have been proposed to predict the squeezing phenomenon. In this article, the potential of squeezing in the Alborz service tunnel was estimated probabilistically by several empirical, semi-empirical and theoretical-analytical methods. In many situations in the Alborz service tunnel route, different methods provided different results. Among these methods, the Aydan *et al.* (1993) method was more accurate in estimating the squeezing phenomenon. Therefore, in this study, 300 data were used to train the ML models and 33 data for test, whose inputs and outputs were determined based on the Aydan *et al.* (1993) method. According to the Aydan *et al.* (1993) method, eight parameters of η_f, η_s, η_p, σ_{ci}, σ_{cm}, γH, $\varepsilon_\theta^\alpha$ and ε_θ^e were considered as the mode's inputs. The obtained results in this study lead to the following conclusions:

As it turns out, the GPR method with the average accuracy of 0.89 has the highest prediction accuracy. Singh *et al.* (1992) and Goel *et al.* (1995) methods also showed good performance with average accuracy of 0.85 and 0.78, respectively. But, as mentioned earlier, given the Singh *et al.* (1992) and Goel *et al.* (1995) methods in Fig. 9, in other situations where squeezing has not occurred, the occurrence probability is high. These methods are very conservative and designing based on these methods can significantly increases the construction costs. The SVR and Aydan *et al.* (1993) methods with accuracies of 0.76 and 0.74, respectively, have provided a good ability to estimate the occurrence of squeezing. The lowest accuracy is provided by the Barla (1995) method, which is equal to 0.27. So, these results showed us that the GPR model can provide a better performance in predicting the squeezing phenomenon than other methods considered in this paper.

- Among the conventional methods the Singh *et al.* (1992), and Goel *et al.* (1995), and Aydan *et al.* (1993) provided a good accuracy with average accuracies of 0.85, 0.78 and 0.74, respectively. The lowest accuracy was provided by the Barla (1995) method, which was equal to 0.27.
- Singh *et al.* (1992), and Goel *et al.* (1995) methods are very conservative and designing based on these methods can significantly increases the construction costs.
- A comparative analysis between the conventional and the ML methods utilized in this study showed that, the GPR model is the most robust model in the prediction of squeezing phenomenon.
- The sensitivity analysis of the input parameters using the MIT method showed that, the most sensitive parameter on the squeezing phenomenon is the $\varepsilon_\theta^\alpha$ parameter with a sensitivity score of 2.18. The sensitivity score for the η_f, η_s, and η_p parameters were less than 1. Therefore, to avoid the complexity of the model and the overfitting problem, it is better to ignore these parameters and only consider five parameters of σ_{ci}, σ_{cm}, γH, $\varepsilon_\theta^\alpha$ and ε_θ^e as the model's inputs. Considering only these five parameters in the ML models, caused the average accuracy provided by the GPR, SVR and ANN methods to increase to 0.92, 0.84 and 0.73, respectively.

- Finally, this article recommends using the GPR model to predict the squeezing phenomenon in tunneling projects.

This work's significance is that it can provide a good estimation of the squeezing phenomenon in tunneling projects, based on which geotechnical engineers can take the necessary actions to deal with it in the pre-construction designs.

References

Aydan, O., Akagi, T. and Kawamoto, T. (1993), "The squeezing potential of rocks around tunnels; theory and prediction", *Rock Mech. Rock Eng.*, **26**(2), 137-163. https://doi.org/10.1007/BF01023620.

Barton, N., Lien, R. and Lunde, J. (1974), "Engineering classification of rock masses for the design of tunnel support", *Rock Mech.*, **6**, 189-236. https://doi.org/10.1007/BF01239496.

Bai, X., Cheng, W.C., Ong, D.E.L. and Li, G. (2021), "Evaluation of geological conditions and clogging of tunneling using machine learning", *Geomech. Eng.*, **25**(1), 59-73. https://doi.org/10.12989/gae.2021.25.1.059.

Fatemi Aghda, S.M., Ganjalipour, K. and Esmaeil Zadeh, M. (2016), "Comparison of squeezing prediction methods: A case study on Nowsoud tunnel", *Geotech. Geol. Eng.*, **34**(5), 1487-1512. https://doi.org/10.1007/s10706-016-0056-0.

Feng, X.T., Zhao, H.B. and Li, S.J. (2004), "Modeling non-linear displacement time series of geo-materials using evolutionary support vector machines", *Int. J. Rock Mech. Min. Sci.*, **41**(7), 1087-1107. https://doi.org/10.1016/J.IJRMMS.2004.04.003.

Ghasemi, E. and Gholizadeh, H. (2018), "Prediction of squeezing potential in tunneling projects using data mining-based techniques", *Geotech. Geol. Eng.*, 1-10. https://doi.org/10.1007/s10706-018-0705-6.

Grelle, G. and Guadagno, F.M. (2012), "Regression analysis for seismic slope instability based on a double phase viscoplastic sliding model of the rigid block", *Landslides*, **10**(5), 583-597. https://doi.org/10.1007/s10346-012-0350-8.

Goel, R.K. (1995), "Correlations for predicting support pressures and closures in tunnels", Ph.D. Thesis, University of Nagpur, India, 310p.

Hoek, E. (1998), "Tunnel support in weak rock", In: Proceeding of regional symposium on sedimentary rock engineering", Keynote address, Symposium of Sedimentary Rock Engineering, Taipei, Taiwan, November 20-22, 1998.

Hoek, E. and Marinos, P. (2000), "Predicting tunnel squeezing problems in weak heterogeneous rock masses", *Tunn. Tunn. Int.*, **32**(11), 45-51. Corpus ID: 130823387

Hoek, E. (2001), "Big tunnels in bad rock", *J. Geotech. Geoenviron. Eng.*, **127**(9), 726-740. https://doi.org/10.1061/(ASCE)1090-0241(2001)127:9(726).

Jethwa, J.L, Singh., B. and Singh, B. (1984), "Estimation of ultimate rock pressure for tunnel linings under squeezing rock conditions—a new approach", (Eds., Brown, E.T. and Hudson, J.A.), Proceedings of ISRM symposium on design and performance of underground excavations, Cambridge, 231-238. https://www.icevirtuallibrary.com/doi/abs/10.1680/dapoue.35652.0028

Kang, F., Han, S.X., Salgado, R. and Li, J.J. (2015), "System probabilistic stability analysis of soil slopes using Gaussian process regression with Latin hypercube sampling", *Comput. Geotech.*, **63**(1), 13-25. https://doi.org/10.1016/j.compgeo.2014.08.010.

Khishe, M. and Mosavi, M.R. (2020). "Chimp optimization algorithm", *Exp. Syst. with Appl.*, **149**, 113338. https://doi.org/10.1016/j.eswa.2020.113338.

Khishe, M. and Mosavi, M.R. (2019), "Improved whale trainer for sonar datasets classification using neural network", *Appl. Acoust.*, **154**, 176-192. https://doi.org/10.1016/j.apacoust.2019.05.006.

Li, L.P., Shi, S.S., Zhang, Q.Q., Zhang, J. and Hu, J. (2017), "Gaussian process model of water in flow prediction in tunnel construction and its engineering applications", *Tunn. Undergr. Sp. Tech.*, **69**, 155-161. https://doi.org/10.1016/j.tust.2017.06.018.

Liu, R., Liu, E., Yang, J., Li, M. and Wang, F. (2006), "Optimizing the hyper-parameters for SVM by combining evolution strategies with a grid search", In: International conference on intelligent computing, Kunming, China, **44**, 712-721. https://doi.org/10.1007/978-3-540-37256-1_87.

Liu, Z.B., Shao, J.F., Xu, W.Y., Chen, H.J. and Shi, C. (2014), "Comparison on landslide non-linear displacement analysis and prediction with computational intelligence approaches", *Landslides*, **11**(5), 889-896. https://doi.org/10.1007/s10346-013-0443-z.

Li, B., Fu, Y., Hong, Y. and Gao, Z (2021), "Deterministic and probabilistic analysis of tunnel face stability using support vector machine", *Geomech. Eng.*, **25**(1), 17-30. https://doi.org/10.12989/gae.2021.25.1.017.

Liu, J., Jiang, Y., Zhang, Y. and Sakaguchi, O. (2021), "Influence of different combinations of measurement while drilling parameters by artificial neural network on estimation of tunnel support patterns", *Geomech. Eng.*, **25**(6), 439-454. https://doi.org/10.12989/gae.2021.25.6.439.

Mahmoodzadeh, A., Mohammadi, M., Abdulhamid, S.N., HIbrahim, H.H., Hama-Ali, H.H., Nejati, H.R. and Rashidi S. (2022). "Prediction of duration and construction cost of road tunnels using Gaussian process regression", *Geomech. Eng.*, **28**(1), 65-75. https://doi.org/10.12989/gae.2021.28.1.065.

Mosavi, M., Kaveh, M., Khishe, M. and Aghababaie, M. (2018), "Design and implementation a sonar data set classifier using multi-layer perceptron neural network trained by elephant herding optimization", *Iran. J. Marine Tech.*, **5**(1), 1-12. http://ijmt.iranjournals.ir/article_31015.html?lang=en.

Mosavi, M., Khishe, M. and Moridi, A. (2016). "Classification of sonar target using hybrid particle swarm and gravitational search", *Iran. J. Marine Tech.*, **3**(1), 1-13. http://ijmt.iranjournals.ir/article_19580.html?lang=en

Mosavi, M.R. and Khishe, M., Hatam Khani, Y. and Shabani, M. (2017), "Training radial basis function neural network using stochastic fractal search algorithm to classify sonar dataset", *Iran. J. Elec. Electronic Eng.*, **13**(1), 100-111. http://ijeee.iust.ac.ir/article-1-959-en.html.

Pal, M. and Deswal, S. (2010), "Modelling pile capacity using Gaussian process regression", *Comput. Geotech.*, **37**, 942-947. https://doi.org/10.1016/j.compgeo.2010.07.012.

Quinonero-Candela, J. and Rasmussen, C.E. (2005), "A unifying view of sparse approximate Gaussian process regression", *J. Mach. Learn. Res.*, **6**, 1939-1959. https://doi.org/10.5555/1046920.1194909.

Rohmer, J. and Foerster, E. (2011), "Global sensitivity analysis of large-scale numerical land-slide models based on Gaussian-Process metamodeling", *Comput. Geosci.*, **37**(7), 91-927. https://doi.org/10.1016/j.cageo.2011.02.020.

Sakurai, S. (1983), "Displacement measurements associated with the design on underground openings", (Ed., Kova´ri, K.) *Proceedings of the international symposium on field measurements in geomechanics*, Balkema, Zurich.

Schulz, E., Speekenbrink, M. and Krause, A. (2018), "A tutorial on Gaussian process regression: Modelling, exploring, and exploiting functions", *J. Math. Psychology*, **85**, 1-16. https://doi.org/10.1016/j.jmp.2018.03.001.

Singh, B., Jethwa, J.L., Dube, A.K. and Singh, B. (1992),

"Correlation between observed support pressure and rock mass quality", *Tunn. Undergr. Sp. Tech*., **7**, 59-74. https://doi.org/10.1016/0886-7798(92)90114-W.

Wang, D.D., Qiu, G.Q., Xie, W.B. and Wang, Y. (2012), "Deformation prediction model of surrounding rock based on GA-LSSVM-markov", *Nat. Sci*., **4**(2), 85-90. https://doi.org/10.4236/ns.2012.42013.

Wenner, D. and Wannenmacher, H. (2008), "Technical challenges during construction of Alborz service tunnel, Iran", Geomechanik und Tunnelbau, **1**(6), 537-542. https://doi.org/10.1002/geot.200800065.

Xiang, G., Ying, D., Gao, C. and Yuan, L. (2021), "Application of artificial neural network for prediction of flow ability of soft soil subjected to vibrations', *Geomech. Eng*., **25**(5), 395-403. https://doi.org/10.12989/gae.2021.25.5.395.

Yuan, J., Wang, K., Yu, T. and Fang, M. (2008), "Reliable multi-objective optimization of high-speed WEDM process based on Gaussian process regression", *Int. J. Mach. Tools Manuf*., **48**, 47-60. https://doi.org/10.1016/j.ijmachtools.2007.07.011.

IC